Polymer 51 (2010) 4948–4957

Contents lists available at ScienceDirect

Polymer

journal homepage: www.elsevier.com/locate/polymer

Transition between crystallization and microphase separation in PS-b-PEO thin film Influenced by solvent vapor selectivity

Ping Yang, Xinhong Yu*, Yanchun Han

State Key Laboratory of Polymer Physics and Chemistry, Changchun Institute of Applied Chemistry, Chinese Academy of Sciences; Graduate University of the Chinese Academy of Sciences, 5625 Renmin Street, Changchun 130022, PR China

ARTICLE INFO

Article history:
Received 14 April 2010
Received in revised form
14 July 2010
Accepted 12 August 2010
Available online 20 August 2010

Keywords:
Microphase separation
Crystallization
Solvent selectivity

ABSTRACT

In this paper, the effect of solvent selectivity on the transition between crystallization and microphase separation of the semicrystalline diblock copolymer polystyrene-b-poly(ethylene oxide) (PS-b-PEO) thin films was investigated. Square-shaped crystals formed due to lower barrier of crystalline nucleation in both poor and good solvent vapor for PEO. However, in poor solvent (cyclohexane) vapor for PEO, crystalline structure changed to microphase separated structure in the square platelets due to the high mobility of PS blocks. Then breakout crystals dominated the morphology of the film. While, in good solvent (water) vapor for PEO, competition between nucleation and dissolution of crystallization caused the formation of imperfect crystals. Then imperfect crystals dissolved due to the high mobility of PEO blocks, and microphase separation dominated the morphology of the film. The gain of free volume of soluble block and the low swelling of crystalline block are keys for microphase separation and crystallization, respectively.

1. Introduction

In recent years, much more attentions have been paid to crystalline-amorphous block copolymers due to the complicated structural pattern and phase transformation process driven by the combined effect of crystallization and microphase separation. Microphase separation and crystallization are the two kinds of coupling between phase transitions in polymer systems. In the case of static coupling, two phase transitions occur sequentially, separated by time or different external fields such as temperature [1]. Alternatively, two phase transitions may take place in the same condition with comparable kinetic rates, which can be regarded as a case of dynamic coupling. The final phase structure depends on the competition between microphase separation and crystallization [2].

Depending on the order–disorder transition temperature, the melting temperature, and the glass transition temperature of the amorphous block, many different morphologies can be generated [3]. Register and his coworkers have reported that microphase separation in semicrystalline block copolymers could be driven by two forces: thermodynamic incompatibility between the blocks in the melt or crystallization of one or more blocks [4]. Furthermore, crystallization behavior of crystalline-amorphous dibolock copolymers has been widely studied [5,6]. Below the order–disorder temperature, block copolymers undergo microphase separation which results in the formation of ordered structure. If the glass transition temperature (T_g) of amorphous blocks is higher than the melting temperature (T_m) of crystalline, a hard nano-confinement can be created [7,8]. The morphology development becomes highly complex when the amorphous block is liquid-like or rubbery during the crystallization process. The early studies on crystalline-amorphous dibolock copolymers ($T_g < T_c$) were mainly carried out on weakly segregated systems, i. e. PCL-b-PB [9], PEO-b-PB [10], and PI-b-PEO [11]. The results showed that breakout crystallization was favor in weakly segregated systems. When the segregation strength of diblock copolyers increased, depending on melt structure and thermal treatment, crystallization may be confined, templated or breakout. Loo et al. [2] and Xu et al. [12] were able to compile a “classification map”. The map classified the regions where the three modes of crystallization were found. The breakout behavior on crystallization was thus observed with $\chi_C/\chi_{ODT} < 3$. By carefully tuning molecular length and temperature, it is possible to control a range of behaviors from pure “breakout” [13].

In most cases, coupling and competition between crystallization and microphase separation were researched in thermal field [1]. The preparation of block copolymer thin films under various solvent evaporation conditions turns out to be a good way to manipulate the microstructure. Many groups have proposed solvent vapor can induce crystallization [14] and microphase

* Corresponding author. Tel.: +86 431 85262267; fax: +86 431 85262126.
E-mail address: xhyu@ciac.jl.cn (X. Yu).

0032-3861/$ – see front matter © 2010 Elsevier Ltd. All rights reserved.
doi:10.1016/j.polymer.2010.08.025

separation [15]. In earlier studies [16–18], the crystals could be broken down simply, and the folded chains of PEO became amorphous or the transition of orientation of crystals. There were few reports about the effect of solvent vapor selectivity on the transition between crystallization and microphase separation, especially, the effect of solvent selectivity on the kinetic complete between microphase separation and crystallization.

In this paper, when PS-b-PEO thin films anneal in solvent vapor, square-shaped crystals of PEO can be observed not only in poor solvent vapor (cyclohexane) for PEO, but also in good solvent (water) vapor for PEO. The crystalline structure can be broken down by microphase separation with increasing of annealing time. The kinetic competition between crystallization and microphase separation during the growth process determines the transition of morphologies. The final state of PS-b-PEO thin film is distinct due to different interactions between PS-b-PEO and solvent vapor.

2. Experimental section

2.1. Materials

The diblock copolymer polystyrene-block-poly(ethylene oxide) (PS-b-PEO, Mn_{PS} = 40000 g/mol, Mn_{PEO} = 35000 g/mol, polydispersity index = 1.04, $T_{gPEO} = -59$ °C) was purchased from Polymer Source Inc. and used as received. The Flory–Huggins segmental interaction parameter between PEO and PS is determined to be $\chi = -7.05 \times 10^{-3} + 21.3/T$ [19]. The degree of polymerization N was calculated on the basis of the equation $N = (\upsilon_{EO}/\upsilon_0)N_{EO} + (\upsilon_{St}/\upsilon_0)N_{st}$, where $\upsilon_{EO} = M_{EO}/\rho_{EO}$, $\upsilon_{St} = M_{st}/\rho_{st}$ and $\upsilon_0 = \upsilon_{EO}\upsilon_{St})1/2$. M_{st} and M_{EO} are the molecular weight of styrene and ethylene oxide monomers, respectively. ρ_{st} = 1.0534 g/cm^3 and ρ_{EO} = 1.1210 g/cm^3 are the densities of amorphous. χN (20 °C) = 56.0.

The solvents, toluene and cyclohexane were bought from Beijing Chemical Reagent Co.

2.2. Sample preparation

The diblock copolymer was dissolved in toluene with concentration of 0.5 wt %. The solution was heated up to 45 °C to obtain clear solution and then spin-coated onto the Si wafers at 3000 rpm for 40 s immediately to inhibit the growth of PEO single crystals in the solutions and precipitate out of the solutions during spin-coating. Prior to spin-coating, the wafers were cleaned with a 70/30 v/v solution of 98% H_2SO_4/30% H_2O_2 at 80 °C for 30 min, then thoroughly rinsed with deionized water and dried. Before removing the residual solvent, the samples were exposed to the saturated cyclohexane and water vapor in the closed vessels at room temperature (20 °C) for different periods, respectively. Then, the samples were removed from the vessel quickly for fast drying.

For a given diblock copolymer, a solvent that is good for one block can be classified as neutral, slightly selective, or strongly selective, according to whether it is good, near Θ, or a non-solvent for the other block. Cyclohexane is a Θ solvent for PS at 34.5 °C [20] ($\chi = -0.556 + 324.3/T$, $\chi_{cyclohexane\text{-}PS} = 0.55$). According to Flory–Huggins theory, polymer and solvent are completely miscible over the entire composition range when $\chi_{P-S} < 0.5$. Although cyclohexane is a poor solvent for PS and PEO [21], the relative affinity of cyclohexane for PS is larger than for PEO appreciably. Water is a good solvent for PEO with χ_{P-S} in the range 0.45–0.48 [22–24] and non-solvent for PS [25], therefore, water is a selective solvent for PEO [26].

2.3. Characterization

The surface morphology of all the films was characterized by atomic force microscopy (AFM) and transmission electron microscopy (TEM). AFM characterization was performed in tapping mode, using a SPA300HV with a SPI3800 N controller (Seiko Instruments Inc., Japan). A silicon microcantilever of which spring constant 2 N/m and resonance frequency ~70 kHz, (Olympus Co., Japan) with an etched conical tip was used for scanning. TEM experiments were performed on TEM-1011 (JEOL Co., Japan) with an accelerating voltage of 100 kV. During the TEM studies, mica was also used as substrate. The samples were placed in a water bath and quickly floated onto the water surface. Pieces of the polymer film were then picked up from the deionized water surface onto copper mesh. In TEM image, the darker region corresponds to the PS domains and the brighter regions to the PEO phase. Instead of staining, reasonable contrast can be achieved due to an electron-irradiation-induce thinning of the PEO [27].

X-ray photoelectron spectroscopy (XPS) spectra were measured with ESCALAB 250 (Thermo electron Co., U. K.) at room temperature by using an Al K_α X-ray source ($h\nu$ = 1486.6 eV). The main chamber of the XPS instrument was maintained at 10^{-9} Torr. The XPS survey spectra obtained at an emission angle of 90°, 63°, 37°, and 10°, respectively. XPS experiments with varying tilting angles are utilized to reveal the detailed microphase-separated nanostructure and the distribution of PS on the film surface. The envelope can be resolved into two chemical components: C–C/C–H at 284.5 eV and ethoxy group carbon in PEO at 286.1 eV. It is readily seen that the larger of the tilting angle, the deeper of the incident thickness. The C1s peak is usually the one which is strongly modified due to the change in chemical environment [28]. The shift in C1s peak position to higher binding energy side is attributed to oxygen contamination of the surface of the films [29–31]. It is normal that the shift in C1s (C–H) peak position around 285 ± 0.5 eV [32,33]. The shoulder peak at large incidence angles (291.6 eV) assigned to C1s ($\pi^* \leftarrow \pi$) [30].

Film thickness in air or solvent vapor was measured by ellipsometer (Jobin Yvon S.A.S Co., France). The film was placed on simple platform of the ellipsometer. Spectroscopic ellipsometry measurements were performed over a wavelength range of 550–800 nm at a fixed incident angle of 70°.

3. Results and discussion

3.1. Initial morphology

AFM image of the as-prepared PS-b-PEO film (thickness is about 30 nm) is shown in Fig. 1. It exhibits an apparent fluctuation with protrusions. Crystalline polymers, such as PEO, are known to retain

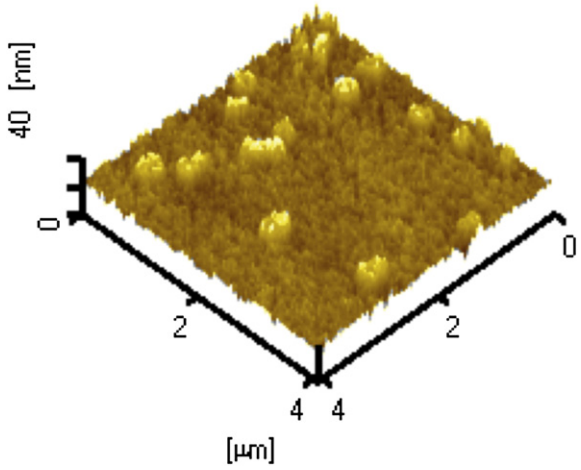

Fig. 1. 3-Dimension AFM topographic image of PS-b-PEO films spin-coated from 0.5 wt % toluene solution onto the Si wafers at 3000 rpm for 40 s.

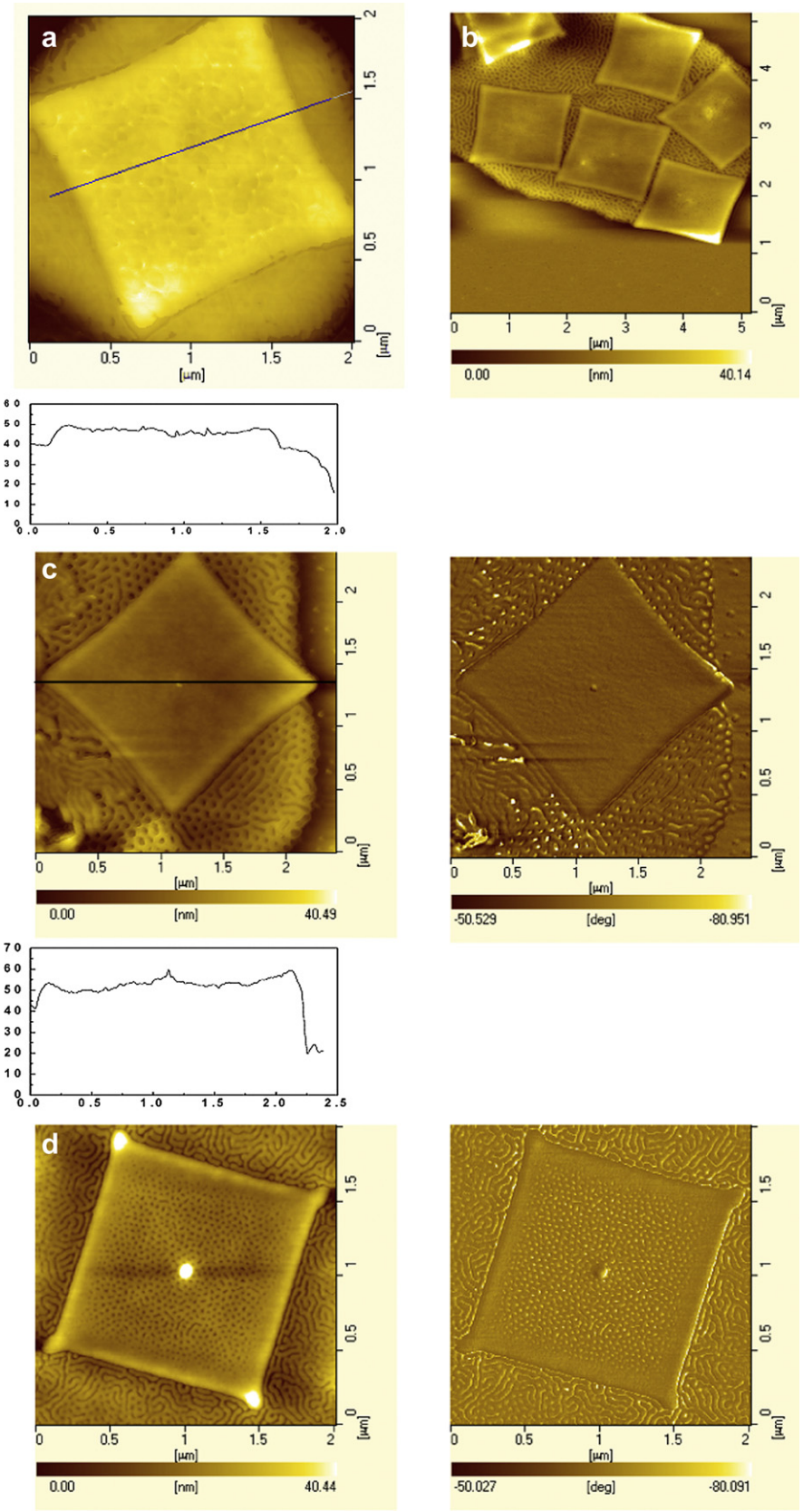

Fig. 2. AFM topographic and phase images of PS-b-PEO thin films in cyclohexane vapor for different times: (a) 1 h, (b, c) 3 h, (d) 48 h, (e) 300 h, (f) 401 h, and (g) 1123 h, respectively.

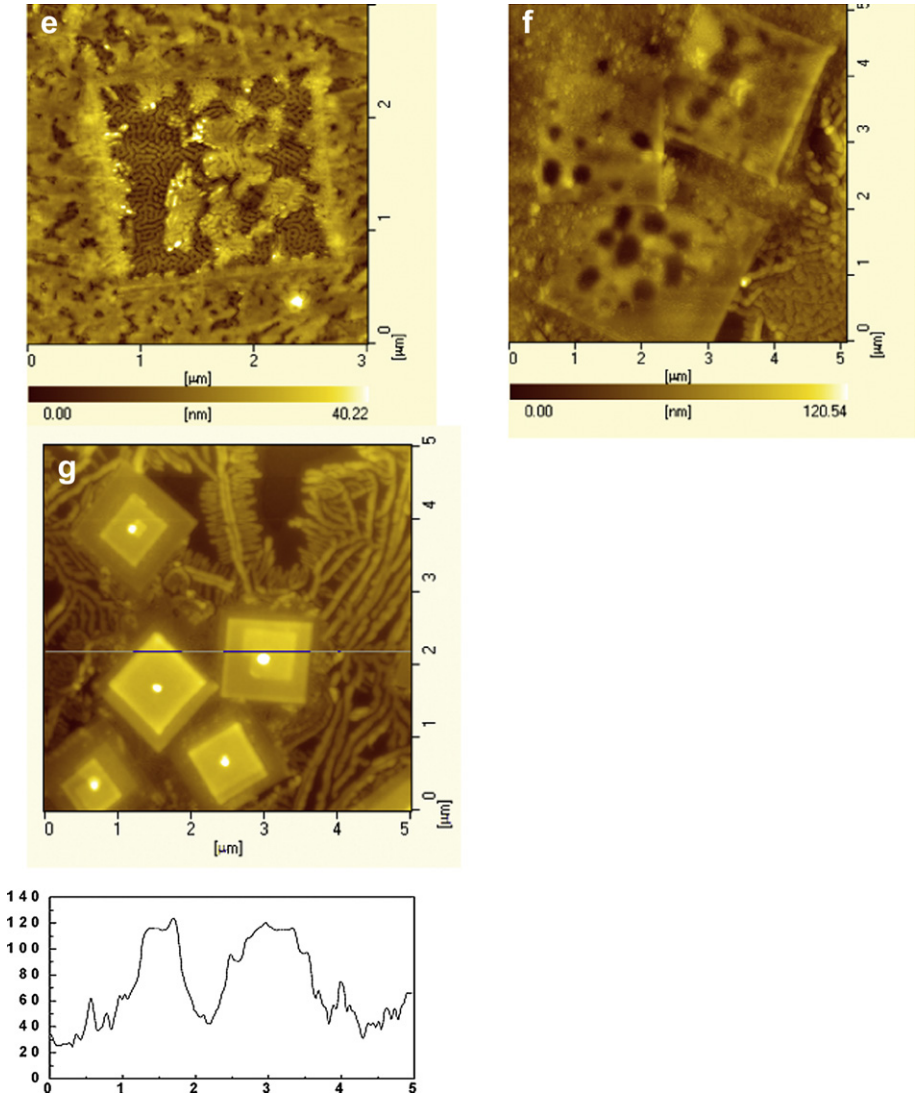

Fig. 2. (*continued*).

some of their crystallinity even in a good solvent and this remaining crystallinity will be a major factor in inducing the formation of aggregates [34]. The PEO blocks tend to form aggregates to avoid contact with toluene in the solution as toluene is a selective solvent for PS [35]. The cores of aggregates are assumed to consist of fold crystallized blocks [36,37]. Thus, the aggregates can be crystalline nuclei.

In solvent vapor, crystallization and microphase separation will occur in semicrystalline block copolymer thin films. In the next section, we show the transition between crystallization and microphase separation of PS-b-PEO film during cyclohexane and water vapor treatment, respectively.

3.2. Morphological transition in cyclohexane vapor treatment

When the as-prepared PS-b-PEO film is annealed in cyclohexane vapor, crystallization changes to microphase separation at first and breakout crystallization occurs subsequently (Fig. 2 and Fig. 3).

After exposure to cyclohexane vapor, square platelets can be observed on terraces (Fig. 2a). They can be further proved by the electron diffraction spots, which are attributed to the two (120) planes (inset of Fig. 3a). The single crystal with chain folding of PEO is "sandwich" covered with the layer of amorphous blocks [38]. With annealing time increasing to 3 h (Fig. 2b,c), microphase separated structure (the mix of lamellar and dots with 40 nm size) occurs around the crystals of PEO on the terrace. The microphase separated structure is confirmed from the phase image that brighter part should represent the PEO domains since the Young's moduli of PS and PEO are 5.2 and 0.2 GPa, respectively [39,40]. The bottom layer becomes flat and featureless (not shown here). It may be a lamellar wetting layer ("brush") [41,42]. For extended annealing time, microphase separation (dots with 20 nm size) also can be observed in the whole surface of the platelets (Fig. 2d). From the TEM image (Fig. 3b) and AFM images of the backside of the structure (Fig. 4), microphase separation can be observed, which suggest that microphase separated structure spans across the platelets and crystalline structure in the platelets is broken down. The conversion process from crystallization to microphase separation with dots morphology means that the increased enthalpy is large enough to overcome the stability of the crystals, but not enough for microphase separation with lamellar morphology.

Subsequently, the growth of breakout crystals of PEO can be observed in the thin film of PS-b-PEO (Fig. 2e). Here, the fingerprint

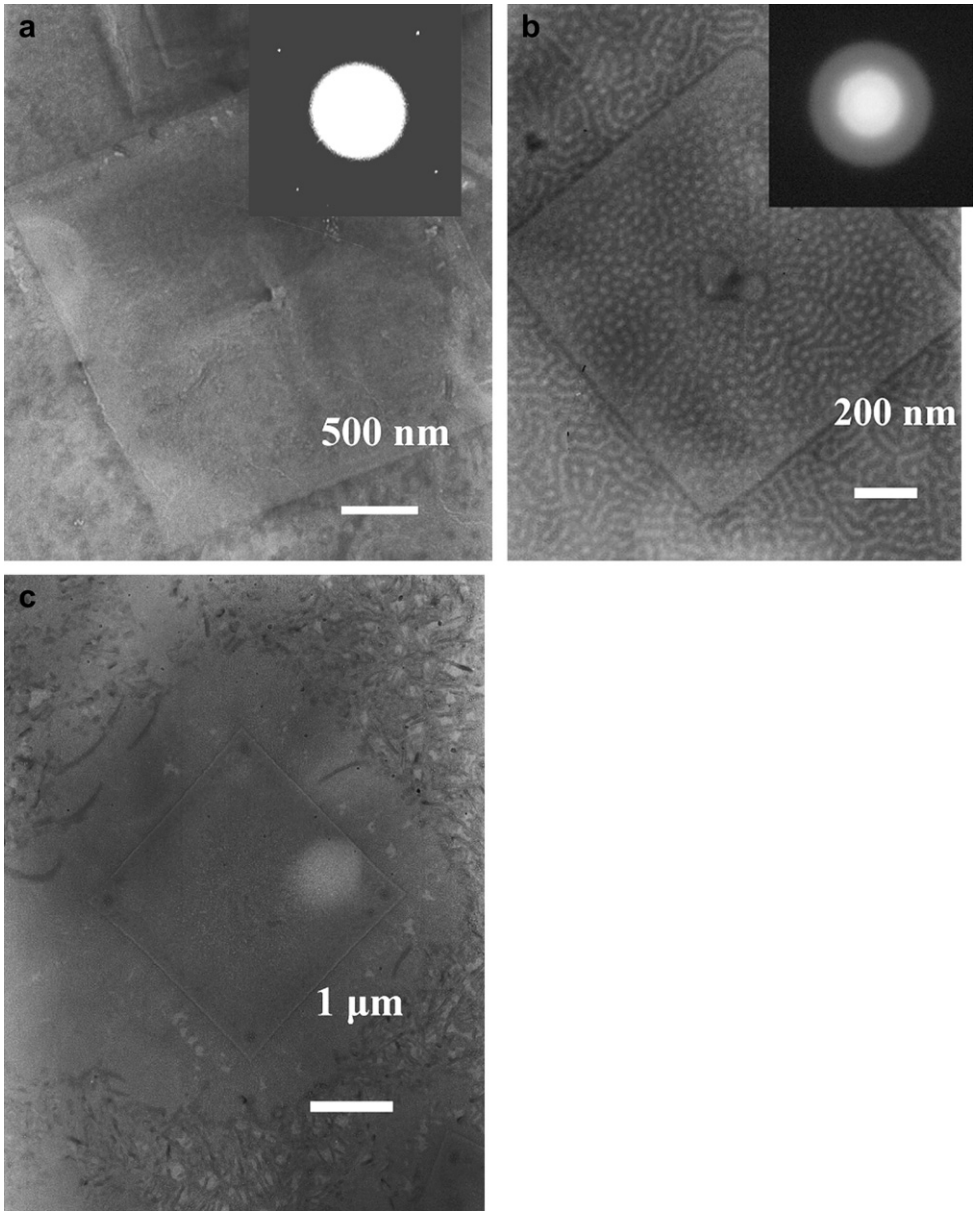

Fig. 3. TEM images of PS-b-PEO thin films in cyclohexane vapor for different times: (a) 1 h, (b) 48 h, and (c) 1123 h, respectively. Inset of (a) shows the selected area electron diffraction pattern. The images were obtained without RuO_4 staining.

structure of breakout crystals is a typical diffusion-limited growth pattern and implies that the morphology is controlled by the diffusion of PEO blocks across PS domains toward the growth [13]. The diffusing process around the square platelets leads to the formation of holes (Fig. 2f) which is similar to the result of thermal annealing [16,17] in the square platelets. Eventually the film is covered by crystals which thickness is about 120 nm (Figs. 2g and 3c). It means that crystallization is more stable than microphase separation in cyclohexane vapor.

3.3. Morphological transition in water vapor treatment

In water vapor, there is a change from crystalline structure to microphase separated structure in square lamella. When PS-b-PEO thin film is annealed in water vapor for 1 h (Fig. 5a,b), square-shaped lamella is found with dendrite-like structure inside [43]. With annealing time increasing to 24 h (Fig. 5c), weak microphase separation occurs on the surface of the square-shaped lamella. For extended annealing time (210 h, Fig. 5d), from the cross-section profiles, the square-shaped lamella moves downward within rims [16,17]. Chains at the boundaries of the crystals are much more mobile as compared with the interior. Existence of square rims means that PEO chains stretch at the edge of crystal and fold more tightly [16]. Meanwhile, microphase separation occurs in the square-shaped lamella (Fig. 5d,e). Different from the film in cyclohexane vapor, there is no lateral microphase separation around the square-shaped lamella.

Eventually, the AFM images (Fig. 5f) and TEM image (Fig. 5g) show small aggregations build up in the film which is representative in previous studies of microphase separation of block copolymer films using AFM [44]. Fig. 6 shows that the binding energy of the C—O peak increases with the increasing thickness, which exhibits PS aggregations distributing in the PEO layer. It has been reported that the phase exhibits the lowest solubility protrudes over the higher solubility phase after solvent removal [45,46].

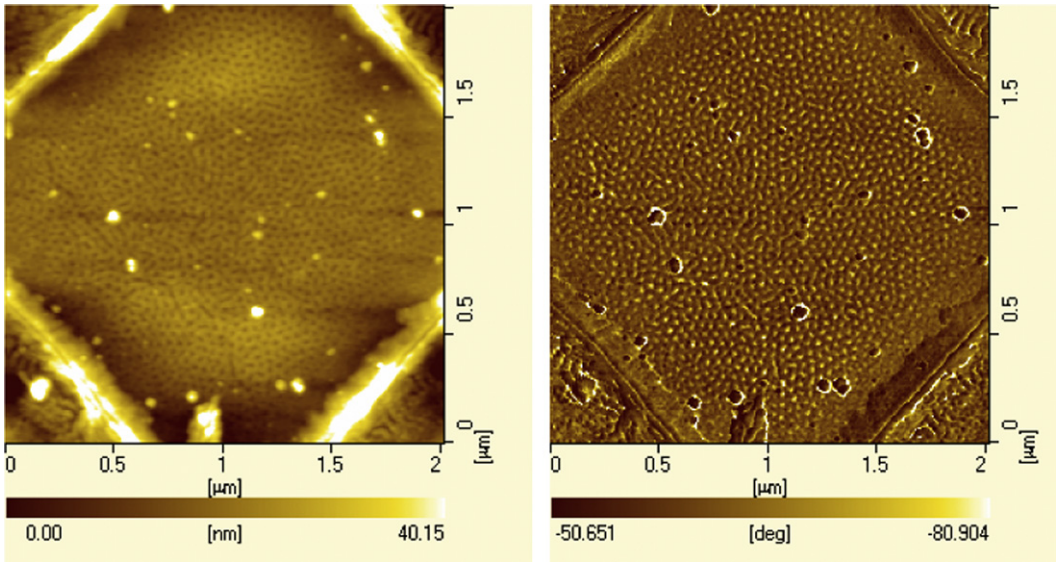

Fig. 4. Typical surface morphology and the corresponding phase contrast AFM images of the backside of PS-b-PEO thin films after annealing in cyclohexane vapor for 48 h.

3.4. Theoretical consideration of the transition between crystallization and microphase separation

The observation of PS-b-PEO thin film annealing in cyclohexane and water vapor is presented in the schematic diagram (Fig. 7). Although a transition from crystallization to microphase separation in PS-b-PEO thin film occurs under cyclohexane or water vapor treatment, there are differences between them.

It has reported the dewetting of block copolymers induced by solvent vapor [47]. When the interaction between one block and the substrate surface (the surface field) is very strong, a stable brush can form. In the case of dense brush, the homopolymer or the same blocks cannot penetrate into the brush deeply, which may lead to autodewetting of the materials [48]. It has reported that the copolymer exhibited autophobic behavior, whereby the top layer dewets a dense "brush" anchored to the silicon substrate [49]. Since the polar PEO layer wets the polar substrate surface preferentially and the PS layer tends to be exposed to the air due to its lower surface energy. When the thin films are annealed in cyclohexane vapor, the film swell (40.7% by volume) and autodewetting occurred. PS-b-PEO block copolymer thin films form terraces on "brush" with energetically favored values of film thickness [50]. The terraces' formation leads to an increase of the film surface and free energy of the system. Since the upper boundary condition still favors the PS, the PS will continue to dominate the upper surface [50]. However, in water vapor, while in the case of lower swelling degree (30.3% by volume) the solvents disturb the film less and thus no dewetting occurred [51]. Therefore, terraces didn't form.

The protrusion in the initial film can act as crystalline nuclei (Fig. 7a). Therefore, the appearance of crystals is prior to microphase separation not only in the poor solvent of PEO vapor, but also in the good solvent of PEO vapor with certain annealing time.

From surface profile analysis (bottom of Fig. 2c), crystals are located on the monolayer ("brush") during cyclohexane treatment. Initially, the crystal is inserted in the films and the thickness of the crystalline structure is about 50 nm and is higher than the terrace about 10 nm (Fig. 2a, Fig. 7b). The resulting "sandwich" crystal structure with amorphous PS layer located at both interfaces is energetically favored [52].

Although PEO crystals prefer to dissolve in water vapor, a small amount of H_2O molecules diffuses into the film initially and the primary role of water is to solvate the PEO blocks by hydrogen bonding and EO facilitates the nucleation of the crystallization of PEO blocks [53]. It also has been reported that crystallization occurs in aqueous PEO solutions because of its regular chain structure [54]. The growth and dissolution of crystallization will compete with each other. Thus, at finite crystal-growth rates, different from the crystals in cyclohexane vapor, only imperfect crystals which thickness is about 30 nm formed in water vapor. In water vapor, no dewetting occurred, and so PEO still existed on the substrate. Therefore, similar to the report [18], heterogeneous nucleation of PEO are predicted to be present predominantly with strong interaction with SiOx substrate and lead to the formation of flat-on lamellae in which the PEO layer is on the surface of silicon and the PS layer is on the top surface of the PEO crystal (Fig. 7b').

The AFM images (Figs. 2a and 5a) show evidence of flat regions around crystals, which indicate incomplete crystallization [55]. The PS component possesses a lower surface energy than that of the PEO block, which leads to parallel lamella around crystals. The strength of phase separation between PEO and PS is determined by χN (χ N (20 °C) = 56.0). Based on the mean-field theory, the incompatibility between PS and PEO is high. The interfacial energy between vapor and film is different from that in air or in vacuum. In cyclohexane vapor, the gain of free volume of the PS blocks induces the increase of enthalpy in the system. Prolonged annealing time in cyclohexane vapor results in sufficient chain mobility of PS chains, so lateral microphase separation can be obtained and the preferential wetting of the PEO block onto the substrate must have reduced the content of the PEO, which would have led to a more asymmetric morphology [56]. The growth of square-shaped crystals is restrained. It is presumed that the increased enthalpy is large enough to change the initial parallel orientation, but not enough for crystal growth of PEO. Therefore, the size of the square-shape crystals are 1–2 μm and a complex structure can be found that single crystals are surrounded by lateral microphase separated structure (Fig. 7c).

The preferential location of microphase separation is different due to the different diffusion process of cyclohexane. When cyclohexane concentration increases in the film, the PS domains swell and PEO crystalline layers do not dissolve. So the diffusivity of solvent molecules in microphase separated domains is higher than in the crystalline domains. Thus, the morphology of microphase

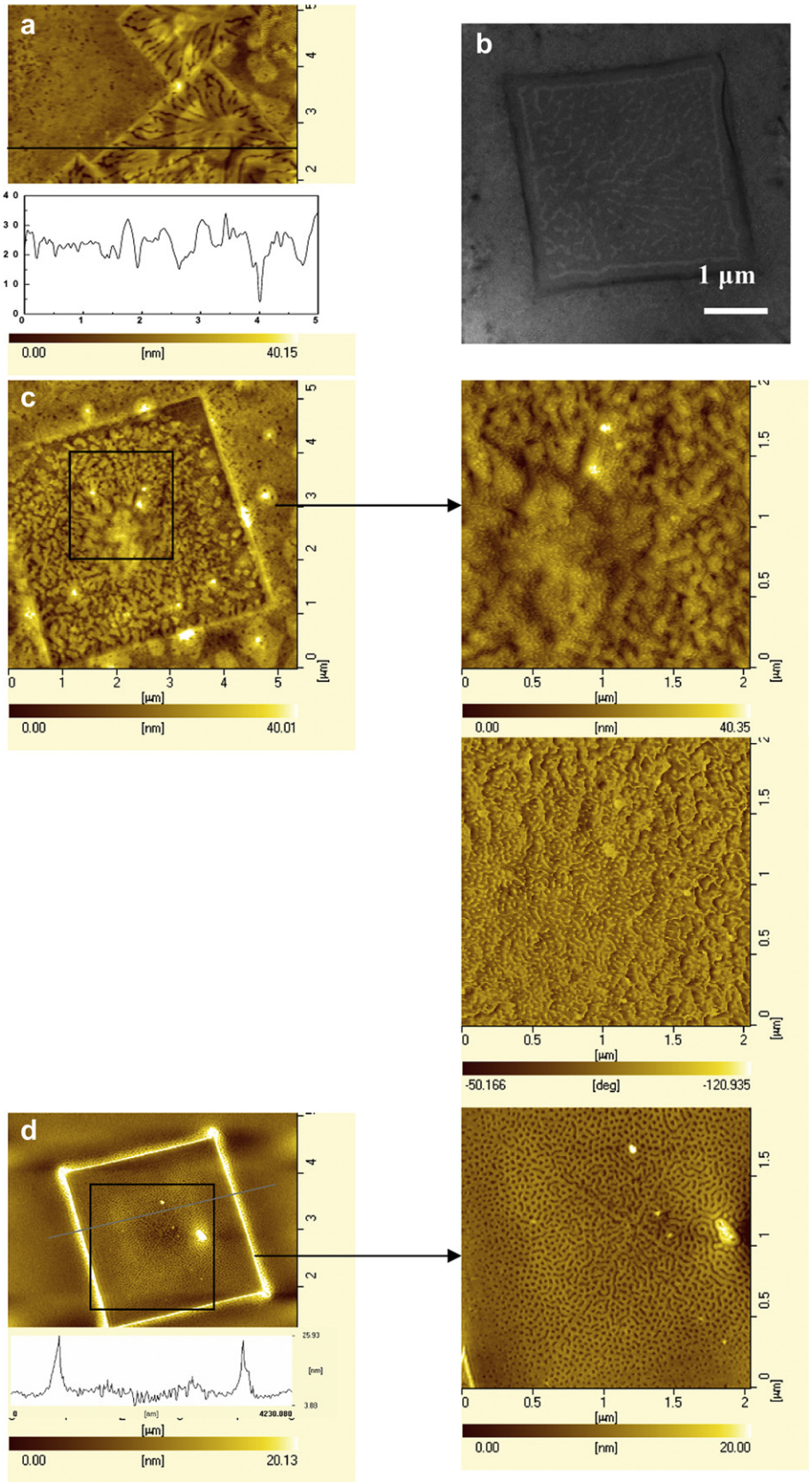

Fig. 5. AFM and TEM images of PS-b-PEO thin films exposed to water vapor for different times: (a, b) 1 h, (c) 24 h, (d, e) 210 h, and (f, g) 401 h, respectively.

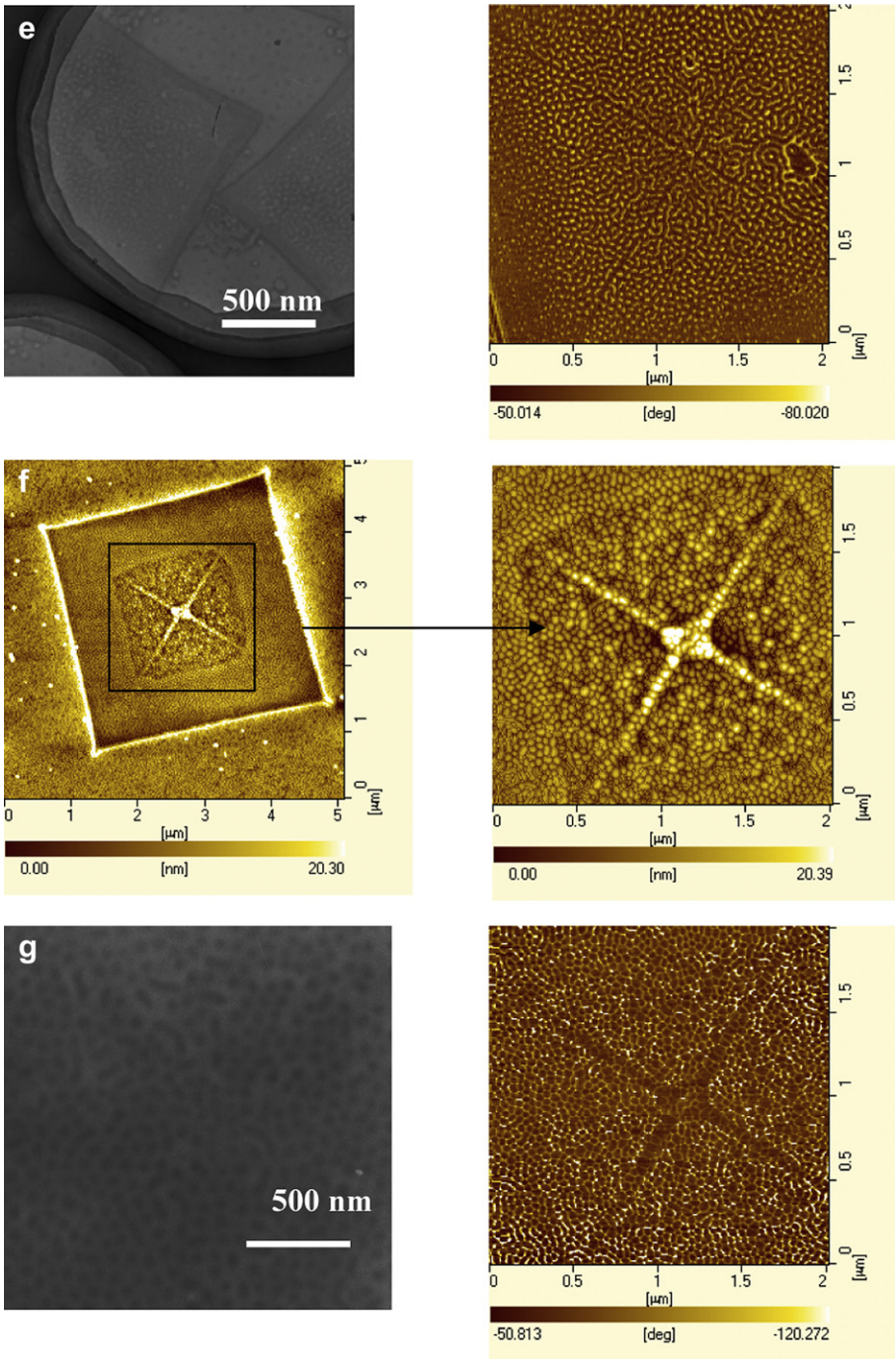

Fig. 5. (*continued*).

separated structure formed around crystals in the film of PS-b-PEO (Fig. 7c). After solvent annealing a certain time, sufficient cyclohexane enters the PEO domains to cause the PEO crystals to dissolve. Therefore, both PS and PEO are highly mobile and can reconstruct themselves easily. Microphase separation can be observed in the whole film.

Different from cyclohexane, water is a selective solvent for PEO at standard temperature and pressure. PS determines water diffusivity in the film, as it may restrict swelling or affect the nature of the PEO phase, which weakens the absorbance of solvent to PEO and hinders the upward movement of PEO. So there is no lateral microphase separation around crystals. The defect of crystal facilitates solvent molecules diffusing. As a result, PS-b-PEO molecules will be rearranged and weak microphase separation take place on the surface of square-shaped lamella firstly. At higher water concentrations, water molecules dissolve the PEO chains, which reduce the driving force for formation of large aggregates. PEO phase within the squared-crystals is fully amorphous and the PEO crystals collapse. We found that polymers at the edges of crystalline domains can relax more easily because at the lateral surface of a crystalline domain the polymers experience fewer constraints—they have fewer neighbors. Consequently, they can reduce their number of chain folds much faster than molecules within such domains. This leads to the formation of a rim (barrier)

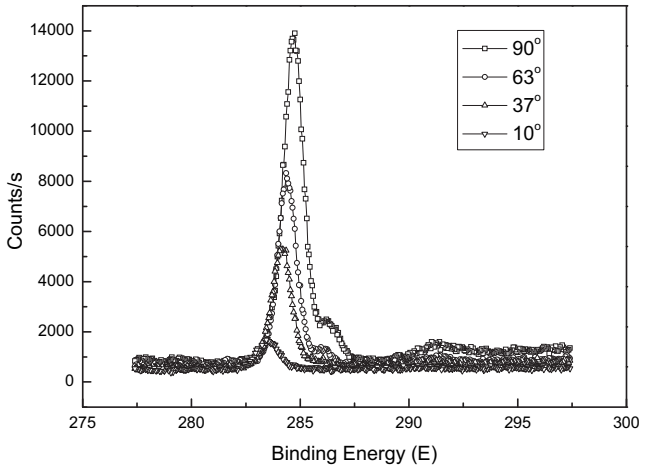

Fig. 6. XPS spectra in the C1 region of the PS-b-PEO thin film treated in water vapor for 401 h.

of less folded polymers where microphase separation occurred even more difficult. The diblock molecules will prefer to self-assemble into microphase-separated morphology within square rims. Thus, cylinders (Fig. 7c') induced by microphase separation form in the square-shaped domains.

In cyclohexane vapor, the happening of local microphase separation inducing fluctuations enhances the instability of the films. Reorganization within polymer crystals can be interpreted as the tendency to remove chain folds. Han et al. [57] demonstrates that the PMMA blocks tend to perforate the PS-rich layer in response to the acetone attraction. Similar to the report, since the relative affinity of cyclohexane for PS is larger than that for PEO, if there is sufficient time for solvation of the entangled PS chains, some PS chains under the platelets tend to perforate the PEO amorphous lamellar in response to the cyclohexane attraction. The diblock molecules will prefer to self-assemble into microphase-separated morphology throughout the platelets with lower free energy (Fig. 7d). The chains at the edge of crystals become more extended and PS segments stretch and move up coupling with PEO segments, thus, the exterior of square platelets are fixed.

Also, PEO blocks tend to perforate the PS-rich layer in response to the water attraction, whereas the PS blocks tend to form aggregates to minimize the unfavorable contact of water molecules with PS chains. Therefore, the PS blocks aggregate to form a spherical core to avoid contact with water and the PEO blocks form a layer around the PS core, resulting in an array of spheres (Fig. 7d').

However, PS matrix is soft in cyclohexane vapor, so the crystallization of PEO block will not be kinetically forced to occur under

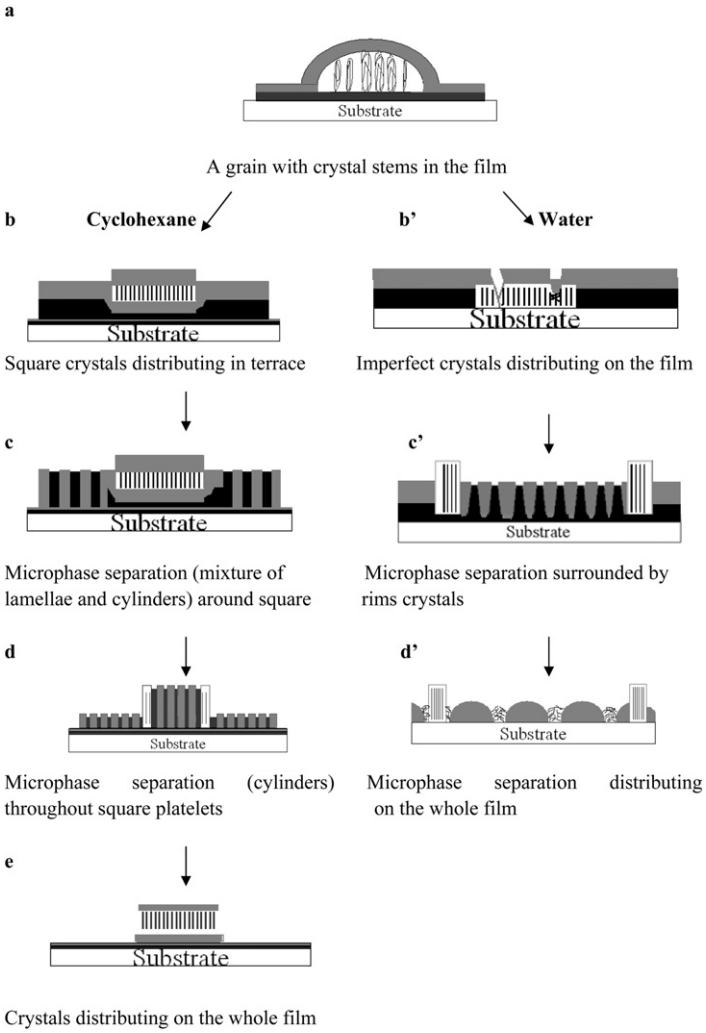

Fig. 7. Schematic illustration of the structure transition of PS-b-PEO thin films in cyclohexane and water vapor for different times. The grey and black lines represent PS chains and PEO chains, respectively.

a physical confinement. It is known that the driving force for crystallization is clearly substantially greater than that for phase separation, so when the film is annealed in the poor solvent vapor of PEO for long time, crystallization dominates [13]. Finally, crystallization dominates over the microphase separation, resulting in the formation of crystals (Fig. 7e).

4. Conclusions

In summary, the transition between crystallization and microphase separation is observed both during poor solvent for PS-b-PEO (cyclohexane) and selective solvent for PEO (water) vapor treatment. Crystallization occurs first due to lower barrier of crystalline nucleation in solution. Solvent vapor selectivity effects the change of morphologies in PS-b-PEO thin film. Herein we report during cyclohexane vapor treatment, microphase separation can occur around square-shaped crystals and then throughout the crystals due to different diffusivity of cyclohexane in the film. Finally, the crystallization energy is larger than the energy associated with microphase separation, so crystallization dominates the morphology of the film. The low swelling of crystalline block plays a key role on crystallization. While in water vapor, the imperfect crystals form due to the competing between nucleation and dissolution of crystals. At higher water concentrations, water molecules dissolve the PEO folded chains, and the PEO crystals collapse within square rims. The attraction between PEO and water, together with the repulsion of PS with the polar PEO and water facilitate the formation of microphase separation. Microphase separation dominates the final morphology of the PS-b-PEO film. The gain of free volume of the soluble block plays a major role on the formation of microphase separation.

Acknowledgment

This work was subsidized by the National Natural Science Foundation of China (20621401, 20923003) and the Ministry of Science and Technology of China (2009CB930603).

References

[1] Li L, Serero Y, Koch MHJ, de Jeu WH. Macromolecules 2003;36:529.
[2] Loo YL, Register RA, Ryan AJ. Macromolecules 2002;35:2365.
[3] Nandan B, Hsu JY, Chen HL. J Macro Sci C Polym Rev 2006;46:143.
[4] Quiram DJ, Register RA, Marchand GR. Macromolecules 1997;30:4551.
[5] Wang L, Meng Z, Yu Y, Meng Q, Chen D. Polymer 2008;49:1199.
[6] Zhang X, Li Y, Zhang C, Hu Y, Song S, Guo H, et al. Polymer 2009;50:5427.
[7] Zhu L, Chen Y, Zhang A, Calhoun BH, Chun M, Quirk RP, et al. Phys Rev B 1999;60:10022.
[8] Huang P, Guo Y, Quirk RP, Ruan J, Lotz B, Thomas EL, et al. Polymer 2006;47:5457.
[9] Nojima S, Kato K, Yamamoto S, Ashida T. Macromolecules 1992;25:2237.
[10] Lee W, Chen HL, Lin TL. J Polym Sci Polym Phys 2002;40:519.
[11] (a) Floudas G, Ulrich R, Wiesner UJ. Chem Phys 1999;110:652;
(b) Floudas G, Vazaiou B, Schipper F, Ulrich R, Wiesner U, Iatrou H, et al. Macromolecules 2001;34:2947.
[12] Xu JT, Turner SC, Fairclough JPA, Mai SM, Ryan AJ, Chaibundit C, et al. Macromolecules 2002;35:6937.
[13] Hobbs JK, Register RA. Macromolecules 2006;39:703.
[14] Harron HR, Pritchard RG, Cope BC, Goddard DT. J Polym Sci Part B 1996;34:173.
[15] Xuan Y, Peng J, Cui L, Wang H, Li B, Han Y. Macromolecule 2004;37:7301.
[16] (a) Reiter G, Castelein G, Sommer JU. Phys Rev Lett 2001;86:5918;
(b) Reiter G.J. Polym. Sci., Part B. 2003; 41: 1869;
(c) Sommer JU, Reiter G. Adv Polym Sci 2005;200:1.
[17] Zhu DS, Liu YX, Shi AC, Che EQ. Polymer 2006;47:5239.
[18] Yang P, Han YC. Langmuir 2009;25:9960.
[19] Zhu L, Cheng SZD, Calhoun BH, Ge Q, Quirk RP, Thomas EL, et al. Polymer 2001;42:5829.
[20] Shula AR, Flory PJ. J Am Chem Soc 1952;74:4760.
[21] Gragson DE, Manes JP, Smythe JE, Baker SM. Langmuir 2003;19:5031.
[22] Mubarekyan E, Santore MM. Macromolecules 2001;34:7504.
[23] Kent MS, Tirrell M, Lodge TP. Macromolecules 1992;25:5383.
[24] Devanand K, Selser JC. Nature 1990;343:793.
[25] Peinmann KV, Abetz V, Simon PFW. Nat Mater 2007;6:992.
[26] Brandrup J, Immergut EH, Grulke EA, Abe A, Bloch DR, editors. Polymer Handbook. 3rd ed. New York: Tohn Wiley & Sons; 1999.
[27] Kim DH, Jia X, Guarini KW, Russell TP. Adv Mater 2004;16:702.
[28] Vandencasteele N, Reniers F. J Electron Spectros Relat Phenom 2010; 178–179:394.
[29] Singha P, Shivaprasada SM, Lala M, Husain M. Solar Energy Mater Solar Cells 2009;93:19.
[30] Thomas HR, O'Malley JJ. Macromolecules 1979;12:323.
[31] Deslandes Y, Pleizier G, Alexander D, Santerre P. Polymer 1998;39:2361.
[32] Brineley A, Davis SS, Davies MC, Watts JF. J Colloid Interf Sci 1995;171:150.
[33] Thomas HR, O'Malley JJ. Macromolecules 1981;14:1316.
[34] Bolls D, Hair ML. J Colloid Interf Sci 1993;157:19.
[35] Peng J, Han Y, Knoll W, Kim DH. Macromol Rapid Commun 2007;28:1422.
[36] Vilgis T, Halperin A. Macromolecules 1991;24:2090.
[37] Yamamoto T. Polymer 2009;50:1975.
[38] Chen WY, Li CY, Zheng JX, Huang P, Zhu L, Ge Q, et al. Macromolecules 2004;37:5292.
[39] Wang H, Djurišić AB, Chan WK, Xie MH. Appl Surf Sci 2005;252:1092.
[40] Nie HY, Motomatsu M, Mizutani W, Tokumoto H. J Vac Sci Technol B 1995;13:1163.
[41] Zhang F, Huang H, Hu Z, Chen Y, He T. Langmuir 2003;19:10100.
[42] Park I, Park S, Park HW, Chang T, Yang H, Ryu CY. Macromolecules 2006;39:315.
[43] Reiter G, Botiz I, Graveleau L, Grozev N, Albrecht K, Mourran A, et al. Lect Notes Phys 2007;714:179.
[44] Huang L, Yuan H, Zhang D, Zhang Z, Guo J, Ma J. Appl Surf Sci 2004;225:39.
[45] Elbs H, Fukunaga K, Stadler R, Sauer G, Magerle R, Krausch G. Macromolecules 1999;32:1204.
[46] Esselink FJ, Dormidontova EE, Hadziioannou G. Macromolecules 1998;31: 4873.
[47] Peng J, Xuan Y, Wang H, Li B, Han Y. Polymer 2005;46:5767.
[48] Li X, Peng J, Wen Y, Kim DH, Knoll W. Polymer 2007;48:2434.
[49] Limary R, Green PF. Macromolucules 1999;32:8167.
[50] Yang P, Han Y. Macromol Rapid Commun 2008;29:1614.
[51] Peng J, Kim DH, Knoll W, Xuan Y, Li B, Han Y. J Chem Phys 2006;125:064702.
[52] Chen DJ, Gong YM, He TB, Zhang FJ. Macromolecules 2006;39:4101.
[53] Polik WF, Burchard W. Macromolecules 1983;16:978.
[54] Huang W, Luo C, Zhang J, Yu K, Han Y. Macromolecules 2007;40:8022.
[55] Li Y, Loo YL, Register RA, Green PF. Macromolecules 2005;38:7745.
[56] (a) Huinink HP, Brokken-Zijp JCM, van Dijk MA, Sevink GJA. J Chem Phys 2000;112:2452;
(b) Huinink HP, van Dijk MA, Brokken-Zijp JCM, Sevink GJA. Macromolecules 2001;34:5325.
[57] Peng J, Wei Y, Wang H, Li B, Han Y. Macromol Rapid Commun 2005;26:738.